NASA Contractor Report 198403

NASA-CR-198403
19960001867

Full-Scale Direct Numerical Simulation of Two- and Three-Dimensional Instabilities and Rivulet Formation in Heated Falling Films

S. Krishnamoorthy and B. Ramaswamy
Rice University
Houston, Texas

S.W. Joo
Wayne State University
Detroit, Michigan

September 1995

Prepared for
Lewis Research Center
Under Grant No. CTS–9408409

National Aeronautics and
Space Administration

FULL-SCALE DIRECT NUMERICAL SIMULATION OF TWO- AND THREE-DIMENSIONAL INSTABILITIES AND RIVULET FORMATION IN HEATED FALLING FILMS [1]

S. KRISHNAMOORTHY[†], B. RAMASWAMY[†] AND S.W. JOO[‡]
[†] Department of Mechanical Engineering and Materials Science
Rice University, Houston, Texas 77251-1892, U.S.A.
[‡] Department of Mechanical Engineering
Wayne State University, Detroit, MI 48202, U.S.A.

A thin film draining on an inclined plate has been studied numerically using finite element method. Three-dimensional governing equations of continuity, momentum and energy with a moving boundary are integrated in an Arbitrary Lagrangian Eulerian frame of reference. Kinematic equation is solved to precisely update interface location. Rivulet formation based on instability mechanism has been simulated using full-scale computation for the first time in the literature. Comparisons with long-wave theory are made to validate the numerical scheme. Detailed analysis of two- and three-dimensional nonlinear wave formation and spontaneous rupture forming rivulets under the influence of combined thermocapillary and surface-wave instabilities is performed.

KEY WORDS: Finite Element Method, ALE Formulation, Spontaneous Rupture, Rivulet, Long-wave Theory

[1]The authors acknowledge the support for this work provided by the National Science Foundation, under GRANT No: CTS-9408409. All computations were performed using Cray-YMP computer at North Carolina Supercomputing Center and NASA Lewis Research Center, Cleveland, Ohio. This work is also partially supported to B.R. by CFD Group at NASA Lewis Research Center through summer faculty fellowship. This research is a part of first author's Ph.D thesis work.

1. INTRODUCTION

The flow of liquid-film on a solid substrate has many significant engineering applications in material processing, biomedical engineering, and nuclear, aerospace and chemical industries. Some of the technological importance are tertiary oil recovery; processes associated with multi-phase flow through porous media; spreading of liquid as in coating process; coalescence of drops and bubbles in foams and emulsion; fabrication of chips in micro-electronics; study of cancer cells; development of anti-icing system for aircraft wings.

The most widely observed phenomena in thin-film flows are those caused by the interfacial instability such as formation of transverse roll waves on the surface, longitudinal roll patterns, wave breaking, rupture, breaking of stream of liquid into independent rivulets, evaporation and termination of liquid layer at a contact line and formation of dry spots Various hydrodynamics forces *viz.* hydrostatic pressure, surface-tension, inertia, thermo-capillary and vapor recoil compete with each other and consequently decide the stability of the system. These instabilities can also be described quantitatively by the film thickness, amount of heating, heat loss at the interface and the angle of inclination of the plane. We follow Goussis and Kelly (1991) and define three modes of instabilities *viz* P-mode, S-mode and H-mode that commonly occur in this type of flow and neglect evaporation, surface contamination and inter-molecular forces. When the plate is tilted, the liquid drains down due to gravity. If the inertia of the mean flow dominates the stabilizing effects of hydrostatic pressure, hydrodynamic or H mode instability sets in. This was identified by Yih (1955) and Benjamin (1957) who formulated linear stability problem by analyzing the growth of spatially periodic two-dimensional disturbances in laminar free-surface flow They arrive at the following condition for neutral stability:

$$\frac{g{d_0}^3 \sin\beta}{2\nu^2} = \frac{5}{4}\cot\beta \tag{1}$$

where, g is the gravitational acceleration, d_0 is the mean film thickness, ν is the kinematic

viscosity of the fluid and β is the angle of inclination. In the limit, as $\beta \rightarrow \pi/2$, $d_0 \rightarrow 0$, *i e.* the flow is always unstable.

When the plate is horizontal and is heated, the interface can be subjected to temperature gradient in any arbitrary orientation. There exists a purely a static base state if the gradient is imposed in the normal direction. Instabilities of this state was first studied by Pearson (1958) and is called as P-mode. If the gradients are imposed along the interface, no static state exists and the thermocapillary can drive a steady shear flow whose instabilities are often times periodic hydrothermal waves (Smith and Davis, 1983a,b). P-mode occurs when the convection is significant and the wavelength of the imposed disturbance is comparable to mean film thickness. The following condition must be satisfied for instability:

$$\frac{d\sigma}{dT}\Delta T\frac{\rho c_p}{\mu \overline{h}} > 32.073 \tag{2}$$

where σ is the surface-tension of the liquid, T is temperature, c_p is the heat capacity, ρ is the density, μ is the dynamic viscosity and $\overline{h}$ is the heat-transfer coefficient. For this mode of instability to develop, the energy transferred to the disturbance and the work done by thermocapillary forces have to be large enough to overcome the losses due to viscous dissipation and surface heat transfer. This mode does not require surface deformation.

S-mode is solely induced by surface deformation when the thickness of the film is small. This was first studied by Scriven and Sterlin (1964). Here, surface-tension suppresses disturbances of shorter wavelength and the film becomes unstable only to long surface waves. The balance between thermocapillary force and stabilizing hydrostatic forces can be expressed as:

$$d_0{}^2\rho g = \frac{3}{2}\left[\frac{-\left(\frac{d\sigma}{dT}\right)\Delta T}{1+\left(\frac{\overline{h}d_0}{\overline{k}}\right)}\right] \tag{3}$$

where $\overline{k}$ is the thermal conductivity of the liquid. As summarized by Goussis and Kelly (1991), at sufficiently thin layers the hydrostatic pressure dominates the effect of inertia and the film is stable with respect to H-mode. As the depth of the layer increases the

inertia dominates and the film becomes unstable. Similarly, for thin layer, the interaction of the basic temperature with perturbation velocity can not transfer enough energy to cause instability. However, in thick fluid layer such transfer of energy is possible and the film is unstable to P-mode. On the other hand, when the layer is thin, thermocapillary dominates hydrostatic pressure and the film is unstable with respect to S-mode However, as the layer thickness increases, due to hydrostatic stabilization, film may become stable In this study, we focus only on S-mode type instability and neglect surface contamination, evaporation and inter-molecular forces.

The presence of both thermocapillary and surface-wave instabilities can cause a heated falling film to rupture and eventually form rivulets. A rivulet is a stream of liquid flowing down a solid surface and sharing an interface with a surrounding gas (Young and Davis, 1987). Hence, it is very important to understand the mechanism of spontaneous rupture before we study the dynamics of rivulet formation. In this regard, we first analyze spontaneous rupture in truly two-dimensional flow and then extend the analysis to three-dimensional rivulet formation.

Theoretically, the combined thermocapillary and surface-wave instability can be studied using linear or weakly nonlinear analysis. Linear stability analysis on these type of flows has been performed since the work of Lin (1975). Kelly *et al.* (1986) identified a "stability window" below and above which the flow becomes unstable due to thermocapillary and surface-wave instability respectively. The window exists due to the stabilizing effects of hydrostatic pressure. Goussis and Kelly (1991) also showed that these instabilities can reinforce each other and a disturbance takes the form of a transverse wave when the film is very thin and a longitudinal roll wave when it is moderately thick. Linear analysis also gives useful information on critical layer thickness, inclination angle, amount of heating and cut off wavenumber for neutral stability. However, we can not follow the dynamics of the flow which is the focus of the present study.

Since the instabilities appear in the form of long interfacial waves, long-wave evolution equation of Benny (1966) type are very useful Burelbach *et al.* (1988) considered sufficiently thin horizontal layer and studied long-wave instabilities in the presence of evaporation, vapor recoil and van der Waals forces. Joo *et al.* (1991) generalized this study to include the effect of mean flow in the absence of van der Waal forces. They studied the nonlinear flow development by numerically integrating the evolution equation. They followed the flow up to the point of rupture when thermocapillary is significant and up to the point of wave-breaking when surface-wave instability is dominant and showed that the rupture always follows a characteristic "fingering" process and substantial local thinning. This process is very sensitive to initial condition. Later on, Joo and Davis (1992) extended the analysis to three-dimensional isothermal flows on a vertical plane and identified a new secondary instability in which three-dimensional disturbance is spatially synchronous with two-dimensional wave. The instability grows for sufficiently small cross-stream wavenumbers and does not require any threshold amplitude. In addition, they studied the three-dimension layers by posing various initial value problems and numerically integrating the long-wave evolution equation. Recently, Joo *et al.* (1995) included thermocapillary also in their analysis and demonstrated a mechanism of rivulet formation solely based on instability phenomenon. They showed that the film first ruptures by "fingering" mechanism and then forms rivulets and when thermocapillary and surface-wave instabilities are properly balanced different flow patterns can be observed. Though long-wave evolution equation can predict the permanent wave form behavior and follow the evolution of finite amplitude disturbances, toward rupture the inertial forces assumed small become significant and the slope of the interface increases continuously. These phenomena eventually violate the basic lubrication type approximation used in long-wave theory formulation. Hence, to study the complicated nonlinear flow development without any *a priori* assumptions, the complete system of Navier-Stokes equations must be solved.

Due to the irregular and time varying domain involved, Finite Element Method is the most popular choice as a numerical tool to investigate thin film flows So far most of the numerical simulations done focus on isothermal flow (Bach and Villadsen 1984; Kheshgi and Scriven, 1987, Ho and Patera 1990; Malamataris and Papanastasiou 1991; Salamon *et al.* 1994; Chippada 1995). Recently Krishnamoorthy *et al.* (1995) have studied rupture dynamics in two-dimensional non-isothermal flows. Bach and Villadsen (1984), Kheshgi and Scriven (1987) and Malamataris and Papanastasiou (1991) use a Lagrangian Finite Element Method to handle moving boundary and control mesh distortion through rezoning. Kheshgi and Scriven (1987) used Galerkin weighted residual, implicit predictor corrector, mixed finite element formulation and studied isothermal thin film flows. Ho and Patera (1990) studied the stability of these flows using Legendre spectral element method. They used Orr-Sommerfeld theory and experimental studies of Kapitza and Kapitza (1949) to compare their spectral element calculations. Salamon *et al.* (1994) used finite element equations written in a reference frame translating at wave speed to study finite amplitude waves propagating at constant speed. They found good agreement with long-wave theory for small amplitude waves, but found their results to qualitatively diverge from long-wave results for large amplitude waves. They also studied the nonlinear interaction between the waves and the secondary subharmonics bifurcation to longer waves. Krishnamoorthy *et al.* (1995) solved the governing equations written in Arbitrary Lagrangian Eulerian frame of reference and showed that in two-dimensional heated film, "fingering" process leading to rupture is not an artifact of long-wave theory but it is an actual phenomena.

In the present study, we the solve complete system of governing equations along with suitable boundary conditions in an ALE frame of reference for both two- and three-dimensional thin-film flows and study the nonlinear flow development to spontaneous rupture and rivulet formation. First, mathematical formulation is discussed in Section (2). The numerical scheme is explained in Section(3). In section(4) results of our simulation

are discussed and comparison with long-wave theory is made wherever possible. Some of the issues that arise during the course of this analysis are discussed and concluded in Section(5).

2. MATHEMATICAL FORMULATION

2.1 Arbitrary Lagrangian Eulerian (ALE) Formulation

Thin film flow problem involves more comprehensive analysis of the local flow pattern and we need to solve free-surface Navier-Stokes equations in primitive variable formulation. We can not impose any ad hoc restriction on the pressure distribution. This results in additional nonlinearities associated with the geometry of the free-surface. To solve the problem more efficiently, we use an arbitrary Lagrangian Eulerian (ALE) frame of reference and write the governing equations accordingly.

The ALE description of the fluid flow is called referential kinematic description of the flow, since the governing equations are written in a frame of reference that move independent of the fluid motion. This formulation was initially proposed by Hirt *et al* (1974) and later on used by many researchers (Chan, 1975, Hughes, Liu and Zimmerman 1981, Ramaswamy and Kawahara 1987, Ramaswamy 1990, Soulaimani *et al.* 1991, Chippada *et al.* 1995) in modeling free-surface flow problems and fluid-structure interaction problems (Donea *et al.* 1982, Donea 1983, Liu *et al.* 1988). ALE formulation has been derived by Donea *et al.* 1982, Ramaswamy and Kawahara (1987), Soulaimani (1991), Lacroix and Garon (1992), among many others and is briefly described next (Chippada 1995).

Let B_0 be the open region occupied by fluid particles at t=0 as shown in Fig.1. This is also called material domain. The position vector of a point P in B_0 is denoted by X_i=(X_1,X_2,X_3). B_t is the open region occupied by B_0 after some time t>0. The point P occupies a unique point p in B_t whose position vector is denoted by x_i=(x_1,x_2,x_3). It is

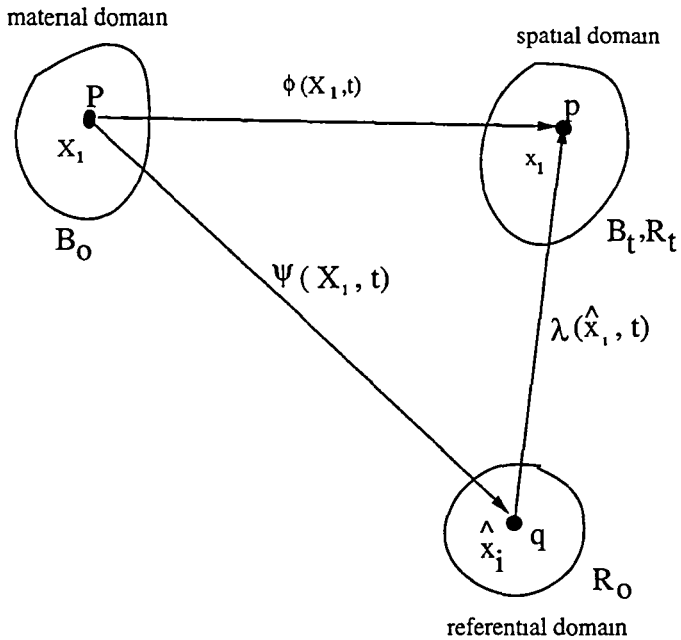

Figure 1: Arbitrary Lagrangian Eulerian description of the flow. Figure adopted from Chippada (1995)

assumed that the mapping between P and p is continuous, unique and invertible

$$x_i = \phi(X_i, t) \quad X_i = \phi^{-1}(x_i, t) \tag{4}$$

Lagrangian (material) velocity is defined as

$$\dot{\phi}(X_i, t) = \frac{\partial}{\partial t}\phi(X_i, t) \tag{5}$$

and Lagrangian acceleration is defined as

$$\ddot{\phi}(X_i, t) = \frac{\partial^2}{\partial t^2}\phi(X_i, t) \tag{6}$$

In terms of spatial coordinate x_i, the Eulerian velocity is defined as

$$u_i(x_i, t) = \frac{\partial}{\partial t}\phi(x_i, t) \tag{7}$$

and the Eulerian acceleration can be shown to take the form:

$$a_i(x_i, t) = u_{i,t}(x_i, t) + u_j(x_i, t)u_{i,j}(x_i, t) \tag{8}$$

Unlike pure Eulerian description, pure Lagrangian description does not involve any nonlinear convective terms. However, Eulerian description is most widely used in fluid mechanics problems

In the ALE formulation, a third domain called the referential domain is specified. At time t=0, it occupies an open region R_0. This body has its own motion and at some time later, t>0, it coincides with the material body which has moved to B_t. That is, the referential point q whose position vector is $\hat{x}_i$=($\hat{x}_1$,$\hat{x}_2$, $\hat{x}_3$) coincides with point p in space coordinate after some time t>0. The mapping between these two regions is given by

$$x_i = \lambda(\hat{x}_i, t) \tag{9}$$

and the referential velocity ($\hat{g}_i$) will be

$$\hat{g}_i(x_i, t) = \frac{\partial}{\partial t}\lambda(\hat{x}_i, t) \tag{10}$$

The relative motion of the fluid with respect to the referential frame is expressed as

$$\hat{x}_i = \lambda^{-1}(x_i, t) = \lambda^{-1}(\phi(X_i, t), t) = \psi(X_i, t) \tag{11}$$

and the relative velocity is

$$\hat{V}_i^{\psi}(\hat{x}_i, t) = \frac{\partial}{\partial t}\psi(X_i, t)\Big|_{X_i} \tag{12}$$

The material point P and the referential point q arrive at the spatial point p through independent motions which are related as follows·

$$x_i = \lambda(\hat{x}_i, t) = \lambda(\psi(X_i, t), t) = \phi(X_i, t) \tag{13}$$

From the above relation, we can derive

$$u_i(x_i, t) = \hat{u}_i(\hat{x}_i, t) = \frac{\partial}{\partial t}\lambda(\psi(X_i, t), t)\Big|_{X_i} \tag{14}$$

$$= \frac{\partial \lambda}{\partial t}(\hat{x}_i, t) + \hat{F}_{ij}(\hat{x}_i, t)\hat{V}_i^{\psi}(\hat{x}_i, t) \tag{15}$$

$$= \hat{g}_i(\hat{x}_i, t) + \hat{F}_{ij}(\hat{x}_i, t)\hat{V}_i^{\psi}(\hat{x}_i, t) \tag{16}$$

where, $\hat{F}_{ij}$ is called gradient deformation tensor defined as

$$\hat{F}_{ij}(\hat{x}_i, t) = \frac{\partial x_i}{\partial \hat{x}_j} \tag{17}$$

The spatial acceleration in the referential coordinates can be shown to be

$$\begin{aligned} a_i(x_i, t) &= \hat{u}_{i,t} + \hat{V}_j^{\psi} \hat{u}_{i,j}(\hat{x}_i, t) && (18) \\ &= \hat{u}_{i,t} + \hat{F}_{ij}^{-1}(\hat{u}_j - \hat{g}_j)\hat{u}_{i,j}(\hat{x}_i, t) && (19) \end{aligned}$$

Comparing spatial acceleration (Eq.8) with referential acceleration (Eq.19), the difference is that gradients are with respect to referential coordinate and the spatial velocity is replaced by the relative velocity. Equation (19) can also be interpreted as material conservation laws with respect to arbitrary moving points. In the event a grid point coincides with the material point, the relative velocity ($\hat{V}_i^{\psi}(\hat{x}_i, t)$) becomes zero Consequently, the set of equations become Lagrangian. Similarly, a pure Eulerian description can be obtained by setting $\hat{g}_i$ to zero. The ALE approach combines the advantages of both Lagrangian and Eulerian methods and avoids mesh distortion. In our problem, the referential motion is related to the fluid motion and at the free boundary, the mesh points are moved normal to the interface with fluid velocity to prevent the loss or gain of fluid material. We use a time stepping procedure in which referential velocity computed from previous time step is used. With this simplification, we write the governing equations.

2.2 Governing Equations

Consider a thin film of Newtonian, incompressible, non-volatile, constant property (density ρ, viscosity μ, thermal conductivity $\overline{k}$, thermal diffusivity α) liquid kept on a plate maintained at a constant temperature T_w and inclined at an angle β to the streamwise direction. The film is thick enough so that the continuum theory is valid and neglect the buoyancy forces. It is unbounded in both streamwise and spanwise directions, but bounded

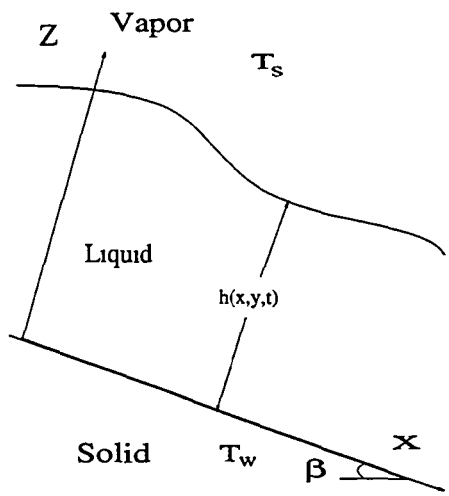

Figure 2: Physical configuration of a thin film flowing down a heated inclined plate (two-dimensional sectional view).

above by a passive gas (having negligible density and viscosity) of far-field temperature $T_s(< T_w)$ and zero pressure. A two-dimensional cross-sectional view of the physical domain is shown in Fig.2. The heat conducted across the liquid layer is lost through the interface due to the convection and affects the interfacial temperature T_i. We assume that surface tension decreases monotonically with temperature:

$$\sigma(T) = \sigma_o \left[1 - \gamma(T - T_s)\right], \tag{20}$$

where σ_0 is the value of the surface tension at the reference temperature T_s and γ is the temperature coefficient. The thermocapillary induced by surface tension gradient is measured by Marangoni number $M{=}\gamma(T_w - T_s)d_0/2\mu\alpha$. In an undisturbed layer of liquid film, the streamwise component of the velocity reaches maximum at the interface and is expressed as $gd_0{}^2\sin\beta/\nu$ where g is gravitational constant, d_0 is the initial mean thickness of the film and $\nu = \mu/\rho$ is the kinematic viscosity of the liquid. The Reynolds number based on the initial maximum velocity and the mean thickness is $G\sin\beta$, where $G{=}gd_0{}^3/\nu$. This is also called Galileo number in some literature. This parameter is a measure of the film thickness.

The governing equations are time-dependent and three-dimensional conservation laws for mass, momentum and energy Using mean film thickness (d_0) and viscous time ($d_0{}^2/\nu$) as the scales of motion, the non-dimensional form of the governing equations in an ALE frame of reference is written as:

$$\mathbf{u}_{i,i} = 0, \tag{21}$$

$$\frac{\partial \mathbf{u}_i}{\partial t} + (\mathbf{u}_j - \mathbf{g}_j)\mathbf{u}_{i,j} = \sigma_{ij,j} + G\delta_{i3} \tag{22}$$

$$\frac{\partial \theta}{\partial t} + (\mathbf{u}_j - \mathbf{g}_j)\theta_{,j} = \frac{1}{P}\theta_{,ii} \tag{23}$$

Here, $\mathbf{u}_i$=(u,v,w) and $\mathbf{g}_i$=(g_x,g_y,g_z) are respectively the velocity vector and the grid-point velocity vector, $P(=\nu/\alpha)$ is the Prandtl number, θ=$(T-T_s)/(T_w-T_s)$ is the non-dimensional temperature, i=1,2,3 and j=1,2,3 , "," denotes the partial derivative and δ_{ij} is the Kronecker delta. The stress tensor σ_{ij} is expressed as:

$$\sigma_{ij} = -p\delta_{ij} + (\mathbf{u}_{i,j} + \mathbf{u}_{j,i}) \tag{24}$$

where p is pressure. The above equations refer to a right-handed Cartesian coordinate system $\mathbf{x}_i$=(x,y,z) whose origin is on the plate, x-axis is aligned with streamwise direction, y-axis runs along spanwise direction and z-axis points normal to the plate into the liquid.

The inclined plate is maintained at a constant temperature T_w and no-slip boundary condition is applied At the liquid-gas interface, z=$h(x,y,t)$, appropriate boundary conditions are applied. They are, the kinematic equation for free-surface motion,

$$h_t + \mathbf{Q}_{i,i} = 0 \quad , \tag{25}$$

balance of normal stress,

$$\sigma_{ij}n_j n_i = 2HS \quad , \tag{26}$$

balance of tangential stresses, for α=1,2,

$$\sigma_{ij}n_j t_i{}^{\alpha} = \frac{M}{P}\theta_{,i}t_i{}^{\alpha} \quad , \tag{27}$$

and the heat balance,

$$\theta_{,t} n_i = -Bi\theta \quad . \tag{28}$$

Here,

$$\mathbf{Q}_i = (\mathbf{Q}_x, \mathbf{Q}_y, 0) = \int_0^{h(x,y,t)} \mathbf{u}_i dz \tag{29}$$

is the volume flow rate vector, n is the unit outward normal vector

$$n_i = (-h_x, -h_y, 1)(1 + {h_x}^2 + {h_y}^2)^{-\frac{1}{2}} \tag{30}$$

and ${t_i}^1$ and ${t_i}^2$ are orthogonal unit tangent vectors to the interface:

$${t_i}^1 = (0, 1, h_y)(1 + {h_y}^2)^{-\frac{1}{2}} \quad , \tag{31}$$

$${t_i}^2 = n_j {t_k}^1 \epsilon_{jki} \quad , \tag{32}$$

H is the mean curvature of the free-surface

$$2H = [h_{xx}(1 + {h_y}^2) - 2h_x h_y h_{xy} + h_{yy}(1 + {h_x}^2)](1 + {h_x}^2 + {h_y}^2)^{-\frac{3}{2}} \quad , \tag{33}$$

M is the Marangoni number, Bi=$(\overline{h} d_0/\overline{k})$ is the Biot number, S=$(\sigma_0 d_0/[3\rho\nu^2])$ is the surface tension number.

The surface-tension enters the dynamics of the problem through the force balance at the free-surface. The normal stress jump at the interface is balanced by surface tension times twice the mean curvature of the interface. In the absence of viscosity this is called Laplace equation which states that the pressure is larger on the concave side of the interface by the amount $2HS$. Thermocapillary is introduced through surface tangential stress balance by the dependence of σ on T. This can either alter the capillary pressure jump at a particular location or introduce surface flow where fluid flows from hot end to cold end (for $\gamma > 0$). Since the bulk of the fluid is viscous, this will also be dragged along. This is known as thermocapillary effect and the instabilities of this type can drive its own instability and does not need any external influence. Biot number Bi determines the amount of heat loss

at the interface Thermocapillary flow does not occur if Bi=0 or ∞. Bi=0 corresponds to insulated free-surface and the interface obtains the plate temperature. On the other hand Bi=∞ corresponds to highly conductive fluid and the interface obtains temperature of ambient gas.

The analysis is done on a three-dimensional box whose base dimensions are $2\pi/k_1$ and $2\pi/k_2$ where k_1 and k_2 are the wavenumbers of the imposed disturbance in the streamwise and spanwise direction respectively. Consequently, periodic boundary condition is imposed for $\mathbf{u}$, p and θ in these directions. In this problem we need to satisfy three hydrodynamic boundary conditions at the free-surface viz , normal stress balance, tangential stress balance and the kinematic equation. We incorporate the normal stress balance directly into the momentum equations and apply the tangential stress balance as a natural boundary. Once the new field variables $\mathbf{u}$, p and θ are calculated, the free-surface height is updated by solving the kinematic equation. This procedure is called kinematic iteration.

3. NUMERICAL SCHEME

The governing equations (21) to (23) along with the boundary conditions are solved using Semi Implicit/Explicit Finite Element Method. In this method, the viscous and pressure terms of the governing equations are treated implicitly and the nonlinear convective terms and the kinematic equation are solved explicitly. The splitting admits the use of fast iterative solvers and helps to minimize storage requirements. This fractional step scheme, based on Helmholtz decomposition theorem proposed initially by Chorin (1968) in finite-difference context, is best suited for the time dependent problem like the present study. Starting with an initial free-surface profile, the first step is to compute an intermediate velocity field ($\tilde{\mathbf{u}}_i^{n+1}$) by omitting the pressure term from the momentum equation. Viscous terms are treated implicitly and the convective terms are treated explicitly. Second-order

Adams-Bashforth Scheme and implicit Euler method are used

$$\left(\frac{\tilde{\mathbf{u}}_i^{n+1} - \mathbf{u}_i{}^n}{\Delta t}\right) + \tilde{\mathbf{u}}_{i,jj}^{n+1} = -\frac{3}{2}(\mathbf{u}_j - \mathbf{g}_j)^n \mathbf{u}_{i,j}{}^n + \frac{1}{2}(\mathbf{u}_j - \mathbf{g}_j)^{n-1} \mathbf{u}_{i,j}{}^{n-1} + \mathbf{F}_i{}^n \qquad (34)$$

Here, i=j=1,2,3 and the contributions from the gravity terms are included in the load vector $\mathbf{F}_i$. Since the diffusion terms are treated implicitly, these terms do not pose any restriction on the stability of the scheme. The time step is chosen such that the CFL condition is always satisfied, *i.e.*

$$\Delta t \leq C \ \min\left(\frac{\Delta x}{|u| + \sqrt{Gh} + \sqrt{\frac{3S}{h}}}, \frac{\Delta y}{|v|}, \frac{\Delta z}{|w|}\right) \qquad (35)$$

where C is the Courant number and $C \leq 1$ for a stable scheme. The terms inside the square root represent the contributions from gravity and capillary waves respectively.

The next step consists of calculating pressure from the intermediate velocity field. This is accomplished by projecting $\tilde{\mathbf{u}}_i^{n+1}$ into a divergence-free space. The resulting pressure Poisson equation is solved by satisfying the normal stress balance at the interface.

$$p_{,ii}{}^{n+1} = \frac{\tilde{\mathbf{u}}_{i,i}^{n+1}}{\Delta t} \qquad (36)$$

After pressure calculation, the final velocity field $\mathbf{u}_i{}^{n+1}$ is computed by adding suitable contribution of the pressure field to $\tilde{\mathbf{u}}_i^{n+1}$

$$\left(\frac{\mathbf{u}_i{}^{n+1} - \tilde{\mathbf{u}}_i^{n+1}}{\Delta t}\right) = -p_{,i}{}^{n+1} \qquad (37)$$

After the final velocity field is computed, the temperature field is calculated by solving the energy equation in similar fashion. In this one step calculation, the convective terms are treated explicitly using second-order Adams-Bashforth scheme and the diffusion terms are treated implicitly using Euler backward method

$$\left(\frac{\theta^{n+1} - \theta^n}{\Delta t}\right) + \theta_{,jj}^{n+1} = -\frac{3}{2}(\mathbf{u}_j - \mathbf{g}_j)^n \theta_{,j}{}^n + \frac{1}{2}(\mathbf{u}_j - \mathbf{g}_j)^{n-1} \theta_{,j}{}^{n-1} \qquad (38)$$

The next step is to locate the free-surface $h(x,y,t)$ that is not known *a priori*. Therefore, at every time-step, we solve the kinematic equation (Eq.25) by assuming the interface as a material surface i e $\mathbf{Q}_z$=0. The limitation of this procedure is that $h(x,y,t)$ needs to be a single-valued function of x and y We solve Eq.25 using Fourier Spectral method. The advantage of using this method over finite-difference/finite element schemes is that this method can preserve the symmetry of the geometry over a very long period of evolution. A specific example is heated thin film on a horizontal solid substrate where the nonlinear flow develops isotropically. The position of the interface is calculated explicitly as:

$$\left(\frac{h^{n+1} - h^n}{\Delta t}\right) + \mathbf{Q}_{i,i}{}^n = 0 \tag{39}$$

Using h^{n+1}, new location $\mathbf{x}_i{}^{n+1}$ of the grid points and grid velocities $\mathbf{g}_i{}^{n+1}$ are calculated. It is assumed that mesh points are resting on vertical spines and are allowed to move only up or down depending on the local interface height. Thus the ability of moving the nodes in the manner we desire is due to solving the governing equations in an ALE frame of reference. Since the grid points are allowed to move only parallel to z-axis

$$\mathbf{g}_z{}^{n+1} = \left(\frac{z^{n+1} - z^n}{\Delta t}\right) \tag{40}$$

and $\mathbf{g}_x{}^{n+1}$ and $\mathbf{g}_y{}^{n+1}$ are always zero. The above procedure is repeated till the film ruptures or the free-surface equilibrates to the desired wave form

4. RESULTS AND DISCUSSIONS

4.1 Rupture Dynamics

We first integrate two-dimensional governing equations to study spontaneous rupture. A simple-harmonic disturbance of the form

$$h(x,0) = 1 + 0\ 1\ \cos(kx) \tag{41}$$

is imposed on the free-surface and its evolution is studied in time (temporal stability analysis). Here, k is the wavenumber of the imposed perturbation. The analysis will be done on one wavelength periodic domain. In this way, we allow the disturbances of wavelength (λ, $\lambda/2$, $\lambda/4$, ...) to grow and interact nonlinearly. This is called as study of super-harmonic instability. Spatial stability analysis, examining growth/decay of a disturbance in space, and temporal stability analysis can be converted into one another through the Gaster transformation. We set k=k_m,$k_m/2$ and $k_m/4$ where k_m is the wavenumber for maximum growth-rate and is defined as $k_c/\sqrt{2}$. k_c is the cut-off wavenumber and is expressed as (Joo *et al.* 1991):

$$k_c = \left\{ \frac{1}{S} \left[\frac{Bi M}{P} \left(\frac{1}{1+Bi} \right)^2 + \frac{2G^2}{15} \sin^2\beta - \frac{G}{3} \cos\beta \right] \right\}^{\frac{1}{2}}. \tag{42}$$

Computation is stopped at any moment when the local film thickness becomes less than 1% of initial mean thickness ($h(x,y,t)$<0.01) and rupture is assumed at that spot. Beyond this point intermolecular forces, neglected in our formulation, become significant. However, in the absence of ionic molecules in the liquid, only van der Waals force of molecular attraction will be significant. This force is destabilizing and the film will ultimately rupture soon.

The computational domain is discretized into non-overlapping three node linear triangular elements. Grid convergence study is conducted for different cases simulated so that we resolve even small scale structures of the flow. In Fig.3 results from one such study is shown for G=1, S=100, P=7.02, M=35.1, Bi=1.0, β=0 and k=k_m. In these figures, snapshot of the interface is shown at different time levels until the film breaks. In (a) we have used 32 modes (33 grid points in the x direction and 11 grid points in the y direction) to solve the kinematic equation. Similarly, we have used 64 and 128 modes respectively in (b) and (c). These figures clearly prove that a grid size of 65 mesh points in the x direction and 11 grid points in the y direction is sufficient. Subsequently, twice or four times this mesh size is used respectively when the wavenumber is $k_m/2$ or $k_m/4$. As it is seen, the spectral method has the advantage that even for coarse grid (33x11), it is moderately accu-

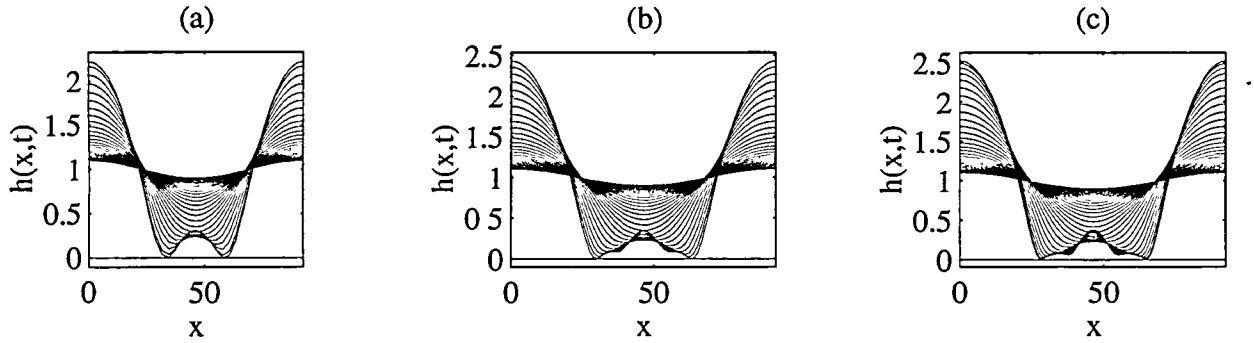

Figure 3: Grid independent study is shown for simulation are G=1,S=100, P=7.02,M=35.1,Bi=1,k=0.0169 and β=0. The mesh sizes are (a) 33 x 11 (b) 65 x 11 (c) 129 x 11

rate enough to preserve the symmetry of the flow geometry. Every problem is highly grid dependent and for different cases studied, different mesh sizes are used to ensure proper resolution of the flow field.

When the film is horizontal, surface-wave instability does not present However, surface tension varies along the free-surface due to the presence of temperature gradient and sets up the Marangoni convection. If the wavelength of the imposed disturbance is sufficiently small and the film is moderately thick, the surface-tension and hydrostatic pressure will stabilize the flow. However, in very thin films, the interface continues to evolve for long surface waves and ultimately ruptures. One such case is shown in Fig 4. The parameters are G=1,S=100,P=7.02,M=106.2, and Bi=0.1 The snapshot of the interface is shown in (a) to (c) for k=k_m,$k_m/2$ and $k_m/4$ respectively. The shape of the free-surface is approximated by a finite Fourier series

$$h(x,t) = \sum_{n=-N}^{N} a_n e^{ikn x} + \text{c.c} \tag{43}$$

and the growth of the first four harmonic modes is shown in (d) to (f) for these cases. Initially, the harmonics grow exponentially as predicted by the linear theory The energy is confined to the fundamental mode and the free-surface maintains its simple-harmonic configuration. As time progresses, thermocapillary becomes significant and thinning of the

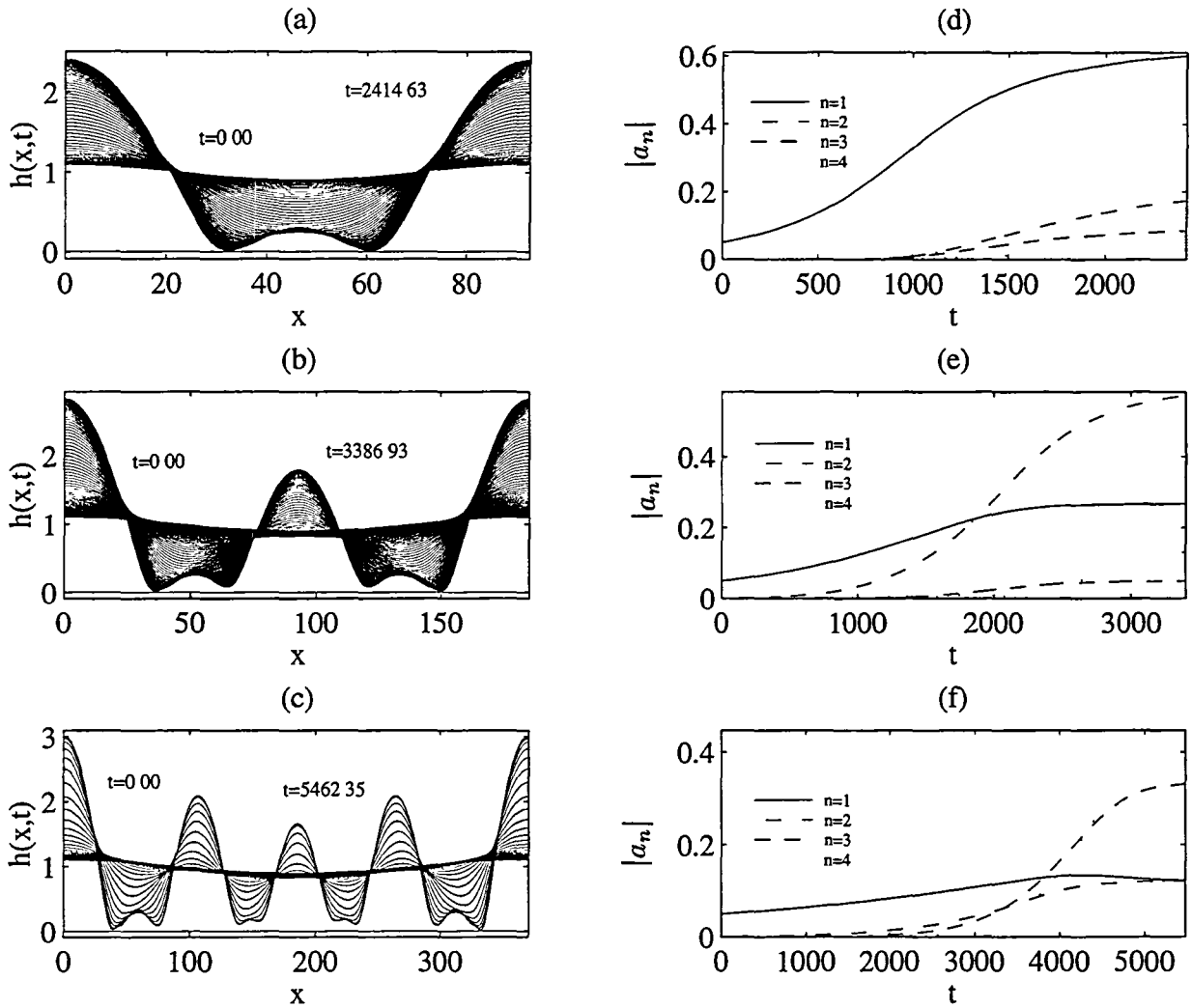

Figure 4: G=1,S=100,P=7.02,M=106.18,Bi=0.1,k_m=0.0677 and β=0. In figures (a),(b) and (c), evolution of the free-surface at the intervals of 100,100, and 200 viscous time units is shown when the disturbance wavenumber is k_m, $k_m/2$ and $k_m/4$ respectively and the corresponding growth in the harmonic modes is shown in (d),(e) and (f). Free surface profile at the point of rupture is also shown along with the rupture time. These results are obtained from finite element simulation.

film continues at the trough. The amplitude of the wave grows and the thin layer of the fluid flattens due to the proximity of the solid wall. The two edges of this flat layer has large slope and very high curvature and are rapidly drawn downwards by the capillary pressure. The pressure of the liquid is lower near the edges than the flat region. This causes the liquid to drain outwards. Meanwhile thermocapillary induces large velocities toward the plate. Consequently, the liquid trapped inside the flat region moves upwards to conserve mass This results in a characteristic bulge at the center. Now the energy is no longer confined to the fundamental mode but has spread to its harmonics as seen in Fig. 4d to 4f. The edges continue to bulge downwards and grow isotropically The growing fingers ultimately touch the plate ($h(x,t)<0.01$) and breaks the film. When the length of the domain is longer ($k=k_m/2$ and $k_m/4$), we can notice several characteristic fingers Finite element mesh at the point of rupture is shown in Fig.5 for these cases

In Fig. 6, the evolution of the interface for the same case from the numerical computation of the long-wave evolution equation (Joo *et al.* 1991) is presented. As the harmonics grow by nonlinear exchange of energy, the Fourier spectrum (Fig. 6d to 6f) broadens to include modes outside long-wave theory. Also, the slope of the free-surface increases rapidly and this violates basic assumptions used in long-wave theory formulation Therefore, this method fails to follow the dynamics up to the point of rupture However, both full-scale and long-wave computations predict formation of fingers before rupture and confirm that the "fingering" process is not an artifact of long-wave theory but indeed an actual phenomenon.

Thermocapillary instability is absent if $Bi=0$ or $Bi=\infty$. When $Bi=0$, the interface temperature (T_i) is same as the temperature of the bottom plate (T_w) and when $Bi=\infty$, T_i is same as the ambient temperature (T_s). Further, Eq.42 shows that $Bi=1$ is the critical value. Consequently, when we increase the Biot number to 1, we increase the thermocapillary and accelerate rupturing process. Krishnamoorthy *et al.* (1995) have already confirmed this by the full-scale direct numerical simulation

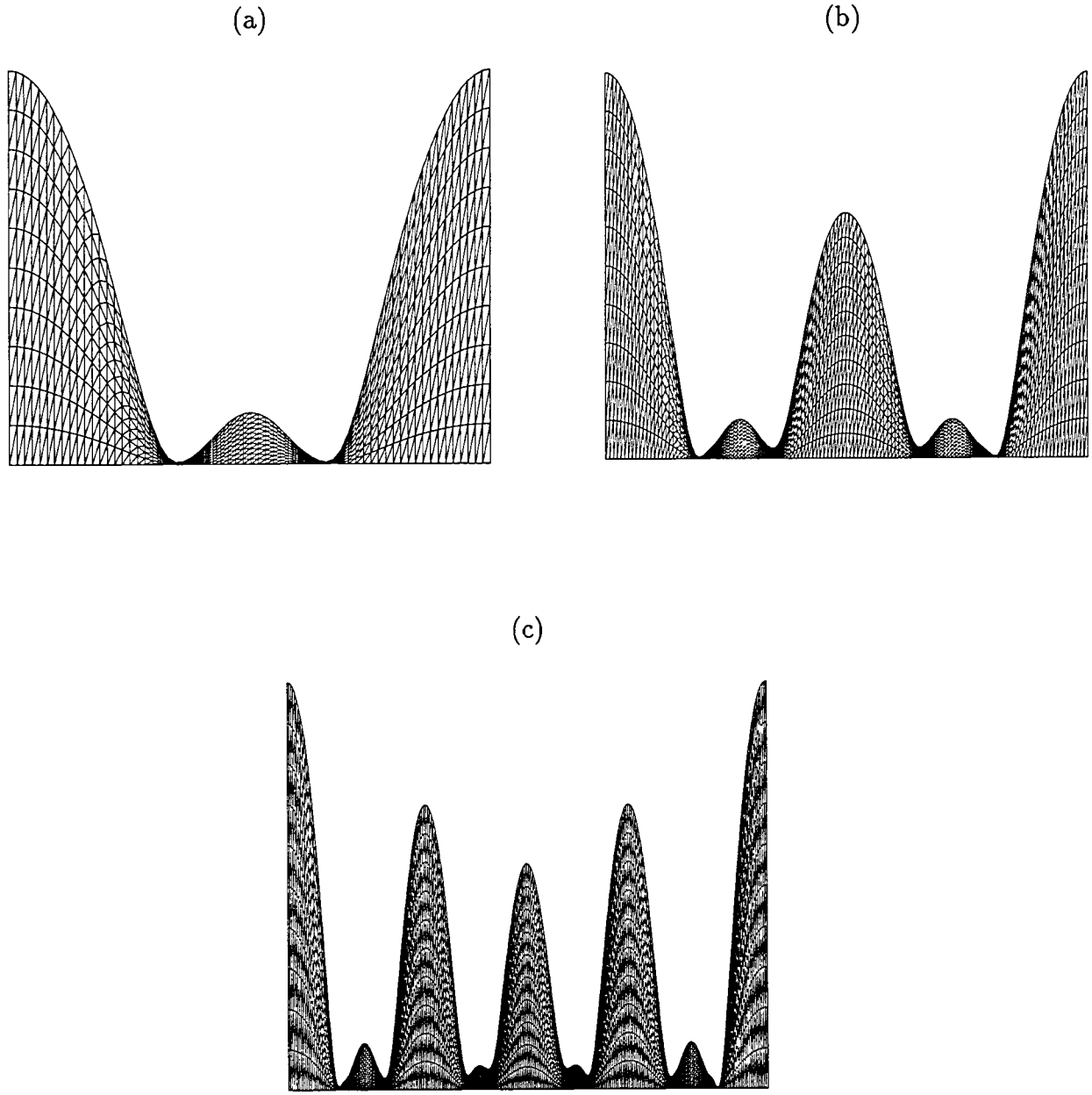

Figure 5: Typical finite element mesh at the point of rupture. The parameters used in the simulation are G=1,S=100,P=7.02,M=106.2,Bi=0.1, k_m=0.0677 and β=0. (a) k_m (b) $k_m/2$ (c) $k_m/4$.

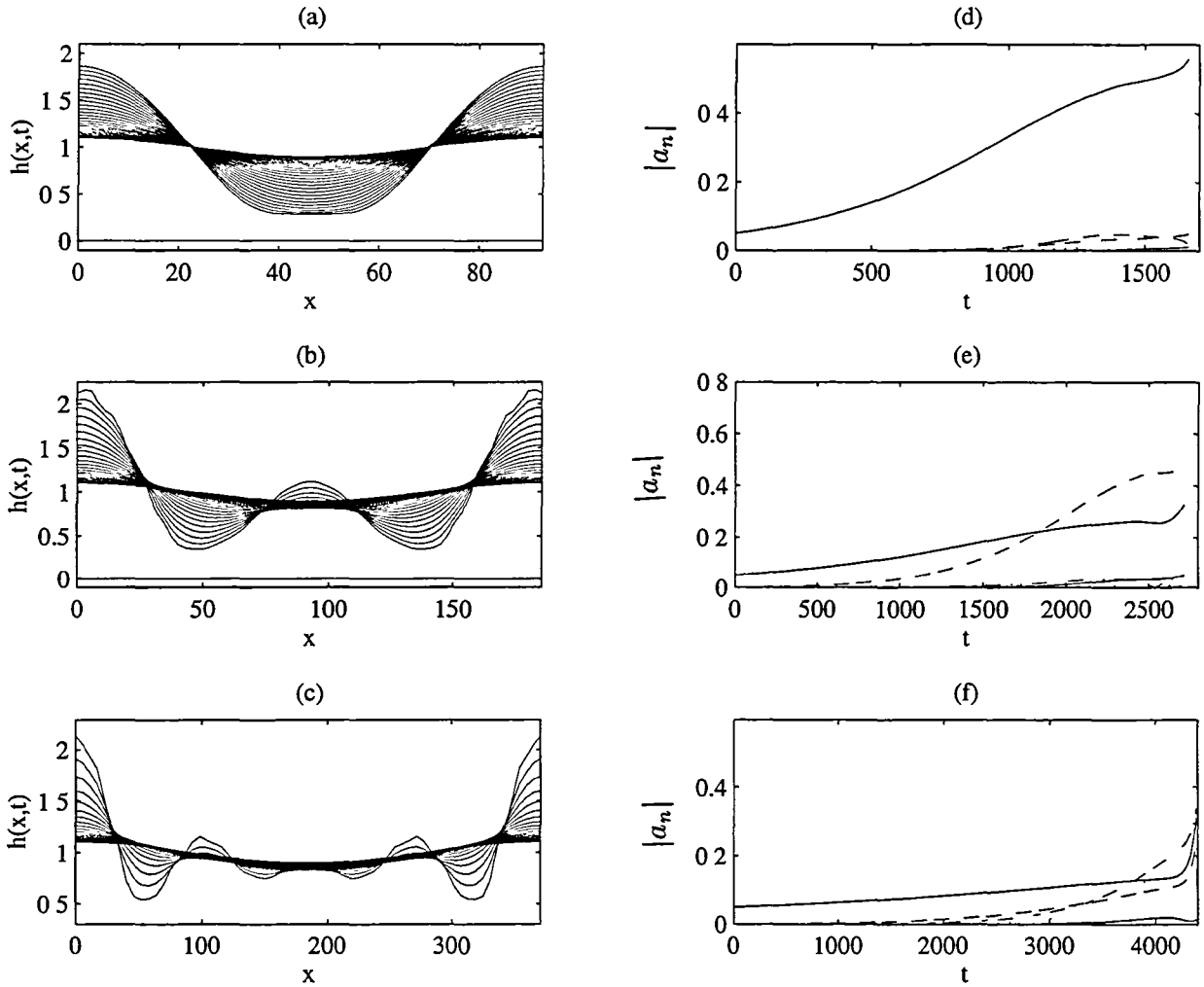

Figure 6 G=1,S=100,P=7.02,M=106.18,Bi=0.1,k_m=0.0677 and β=0. In figures (a),(b) and (c), evolution of the free-surface at the intervals of 100,100, and 200 viscous time units is shown when the disturbance wavenumber is k_m, $k_m/2$ and $k_m/4$ respectively and the corresponding growth in the harmonic modes is shown in (d),(e) and (f). These results are obtained from the spectral calculation of long-wave evolution equation (Joo *et al.* 1991)

When the plate is tilted, i.e., $\beta > 0$, the effect of the mean flow is present. Joo *et al.* (1991) have showed that when there is no surface-wave instability and thermocapillary is weak, the flow equilibrates after initial instability. When the surface-wave instability is present, thermocapillary enhanced this instability and promotes wave breaking. When the thermocapillary is strong, the disturbance grows continuously and results in rupture. In Fig. 7, thin film flowing down on a vertical plate is shown when G=5,S=100,Bi=0.1,P=7 and M=70. In this case there is no hydrostatic stabilization and the flow is driven by gravity. Initially, the harmonics grow exponentially as per linear theory. As time progresses, there is a nonlinear exchange of energy among the modes and since thermocapillary is weak, the surface-wave instability causes the film to saturate to a permanent wave form. However, for k=$k_m/4$, the film never saturates and there is a continuous exchange of energy among the modes. This also indicates the influence of wavenumber on the nonlinear flow development. Evolution of the spectral coefficients shows that at t=1138.31, the mode n=$\pm$2 dominates and the wave has two peaks In Fig. 8, we increase the thermocapillary (BiM/P=10) and reduce the surface-wave instability (G=1). Due to the strong thermocapillary instability, the film never saturates, but continue to develop and breaks.

4.2 Rivulet formation

We solve an initial value problem by imposing a simple-harmonic disturbance of the form

$$h(x,y,0) = 1 + 0.1\cos(k_1 x) + 0.1\cos(k_2 y) \tag{44}$$

where k_1 and k_2 are respectively the streamwise and the spanwise wavenumber of the disturbance such that k=$\sqrt{{k_1}^2 + {k_2}^2}$. We integrate three-dimensional governing equations and examine the evolution of the perturbation in time. The analysis will be done on one spatial period box whose base dimension is ($2\pi/k_1$,$2\pi/k_2$). The growth of subharmonics, that can occur in laboratory situation, is not allowed. We select k such that $k < k_c$ where

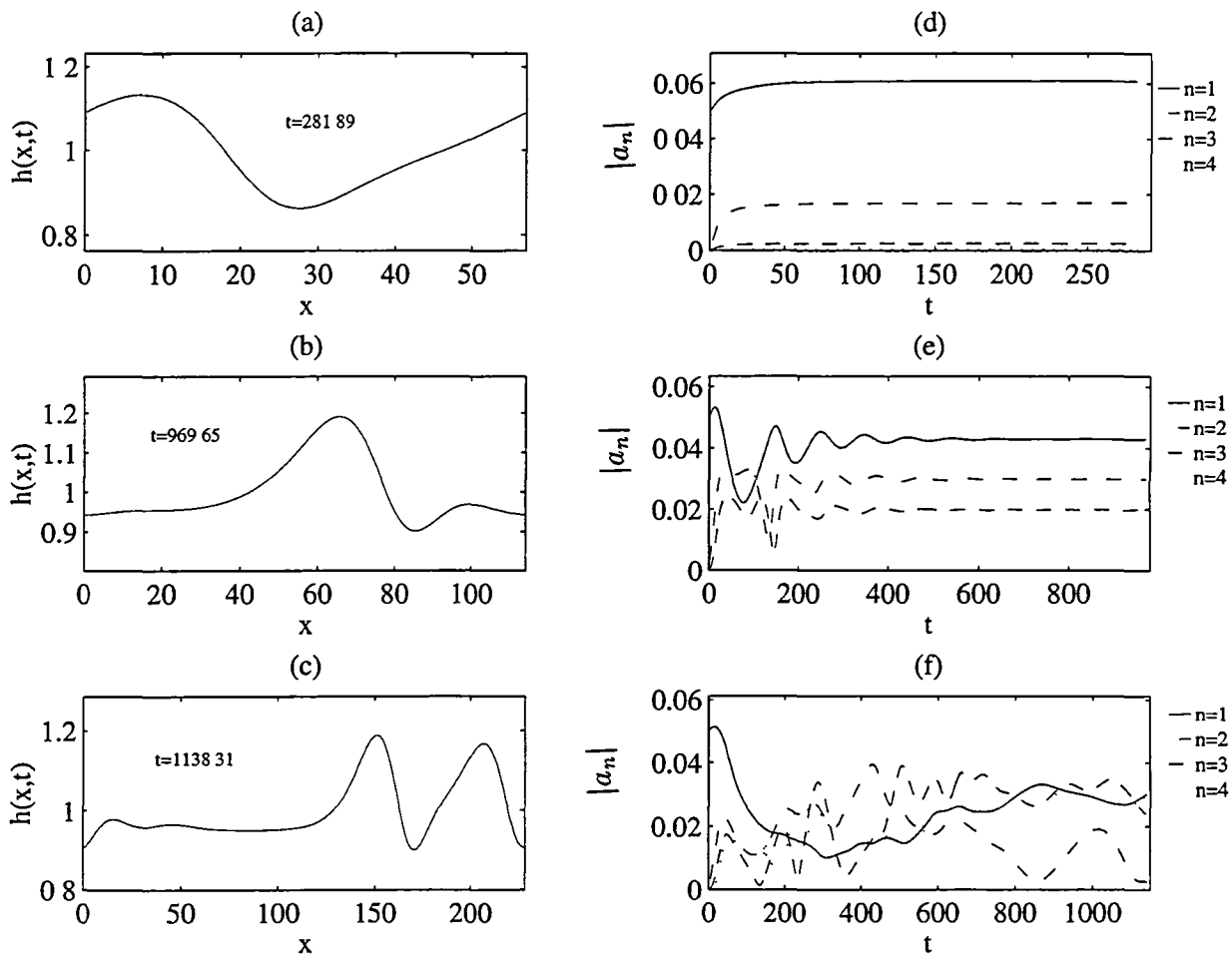

Figure 7: G=5,S=171,P=7,M=70,Bi=0.1,k_m=0.1103 and β=90. In figures (a),(b) and (c), the free-surface shape is shown for the time indicated when k=k_m,$k_m/2$ and $k_m/4$ respectively. Corresponding growth in the harmonic modes during this period is shown in (d),(e) and (f). These results are obtained from finite element simulation

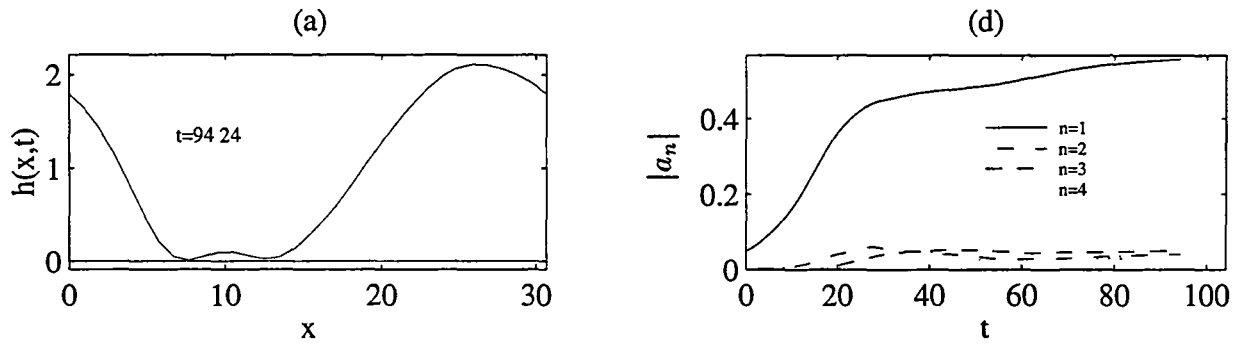

Figure 8: G=1,S=100,P=7,M=700,Bi=0.1,k_m=0.2049 and β=90. In figure (a), the free-surface shape at the point of rupture and in (b) evolution spectral coefficients are shown for k=k_m. These results are obtained from finite element simulation.

k_c is the cut-off wavenumber and is expressed as (Joo *et al.* 1993):

$$k_c = \left\{ \frac{1}{S} \left[\frac{BiM}{P} \left(\frac{1}{1+Bi} \right)^2 + \frac{2G^2}{15} \sin^2\beta \cos^2\theta - \frac{G}{3} \cos\beta \right] \right\}^{\frac{1}{2}}. \tag{45}$$

We stop the computation at any moment when the local film thickness becomes less than 0.01 and rupture is assumed at that spot. Beyond this point intermolecular forces, neglected in our formulation, become significant. As explained in § 4.1, these forces are destabilizing and ultimately break the film. The computational domain is discretized into non-overlapping four node linear tetrahedral elements such that six of these elements make one cubic box.

When the film is vertical, the flow is driven by gravity and hydrostatic pressure does not present. Thermocapillary and surface-wave instabilities can enhance each other and the film flow may saturate or rupture depending on which mode of instability is dominant. In our simulations, the plane is inclined only in the streamwise direction. Consequently, there will not be any mean flow in the spanwise direction. In Fig.9a to 9e evolution of a vertical falling film is shown for t=150, 300, 600, 970 and 1027 respectively when G=1, S=100, Bi=1, M=35 and P=7. In each figure, the free-surface shape, contour plot of interface height predicted by finite element calculation and spectral computation of long-wave theory are shown in order. The wavenumbers of the initial disturbance are k_1=k_2=0.5.

Initially, as the liquid drains downward, surface-wave instability is dominant and the flow evolves downstream and is shown in Fig. 9a. Here, the local phase speed of the layer is proportional to its thickness as per linear theory. As time progresses, the local thinning of the liquid layer persists (Fig. 9b at t=300). Now thermocapillary begins to dictate the growth of the liquid layer and the transverse wave is affected by the three-dimensional instability. In the absence of mean flow in the spanwise direction, the liquid is displaced laterally (Fig.9c) by thermocapillary instability. This process is similar to the evolution of a heated thin film on a horizontal substrate. The "thin layer" effect causes the fingers to grow and a three-dimensional longitudinal pattern (rivulet) develops along the centerline of the stream. At t=970 (Fig.9d), all the superharmonics are excited by this nonlinear exchange of energy and the long-wave theory is no longer valid beyond this point. However, using full-scale computation, we can integrate the governing equations all the way to rupture. The final state is shown in Fig.9e. This simulation confirms Joo *et al.*(1995) observation that the longitudinal rivulets aligned with the mean flow can form only when both the thermocapillary and surface-wave instabilities are properly balanced and neither of these two instabilities alone has the tendency to develop such pattern. This simulation also explains a mechanism for rivulet formation from purely a stability point of view.

In Fig.10a to 10c, the evolution of the thin film is shown for spanwise wavenumber k_2=0.25 for various time levels indicated. All other parameters are identical to the previous case. In this case local thinning rates are smaller and so the rupture time is increased. However, "fingering" occurs in an early stage of the evolution and the rivulets are much larger.

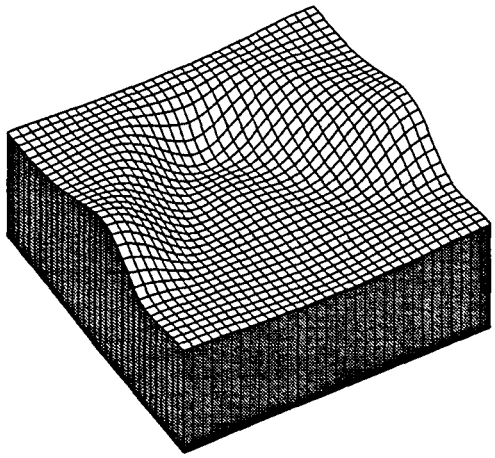

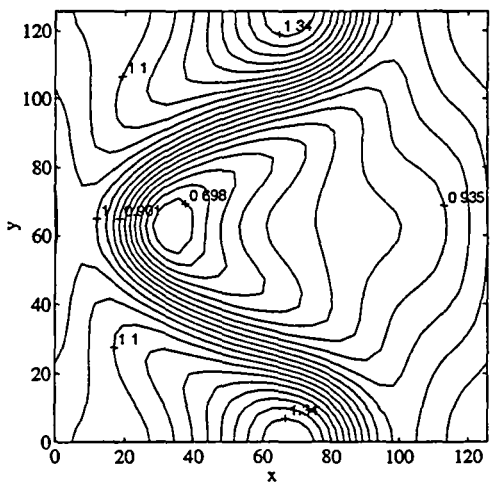

(FEM)

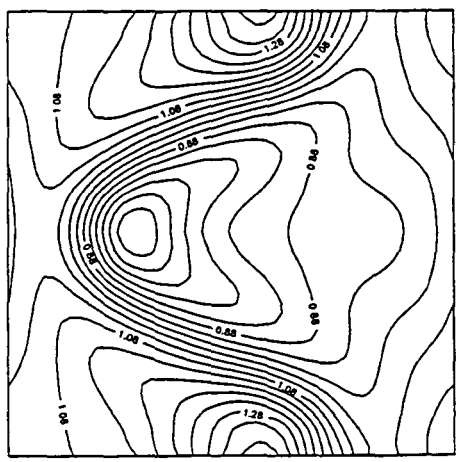

(Long-wave theory)

(a) t=150

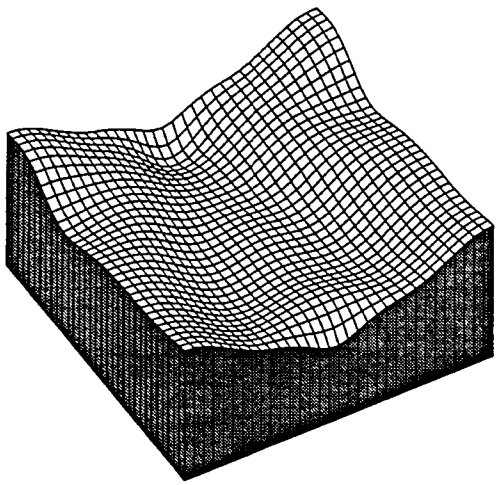

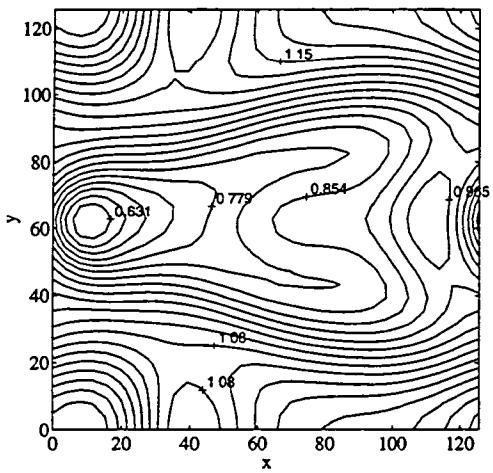

(FEM)

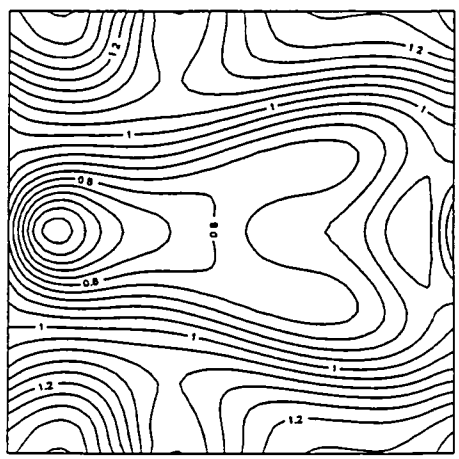

(Long-wave theory)

Figure 9 (b) t=300

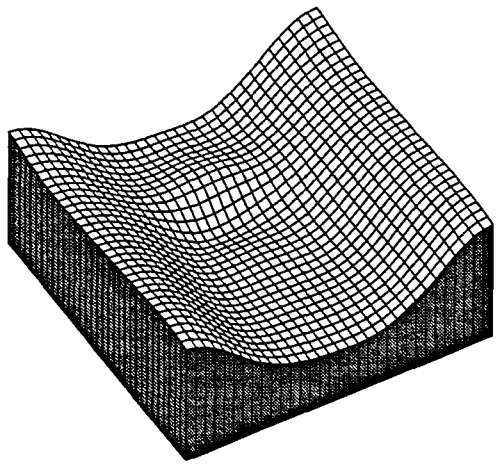

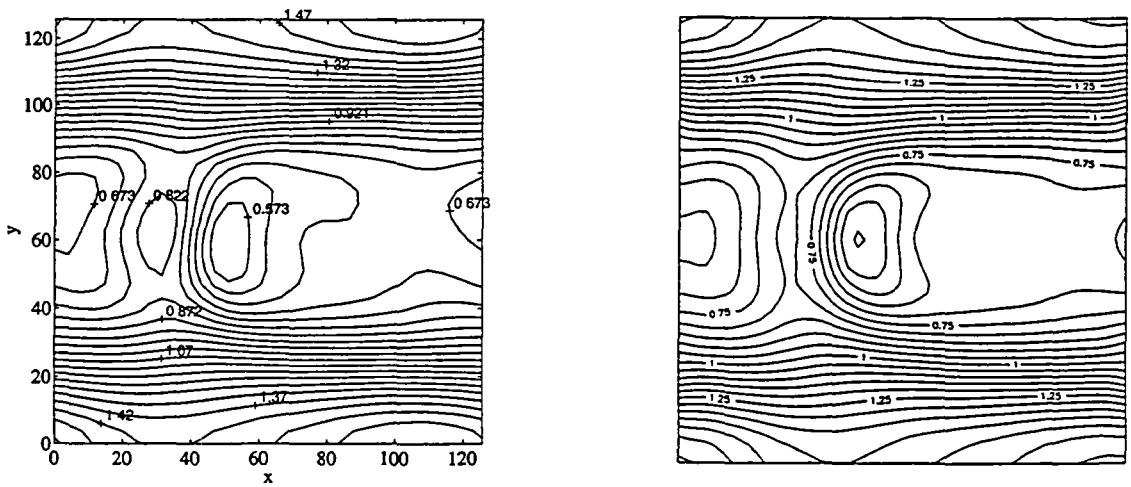

(FEM) (Long-wave theory)

Figure 9 (c) t=600

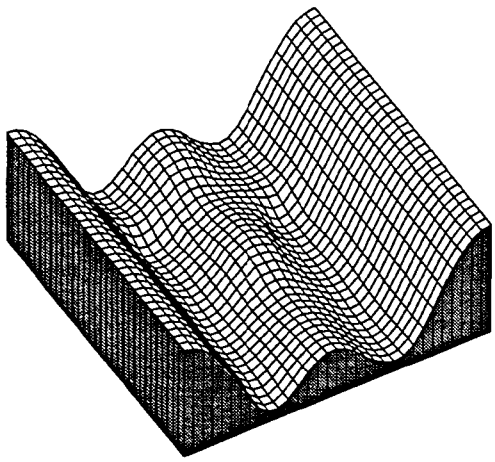

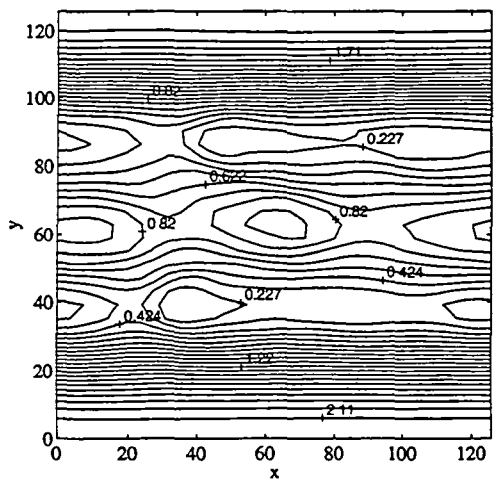

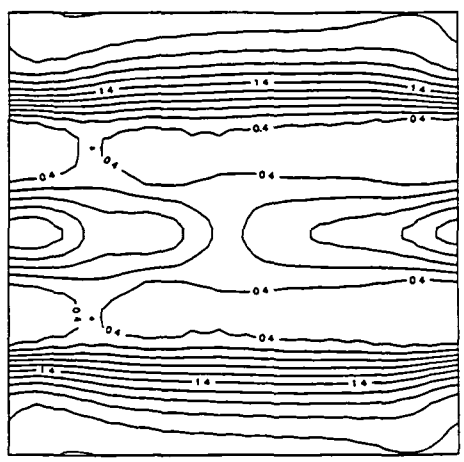

(FEM)

(Long-wave theory)

Figure 9 (d) t=970

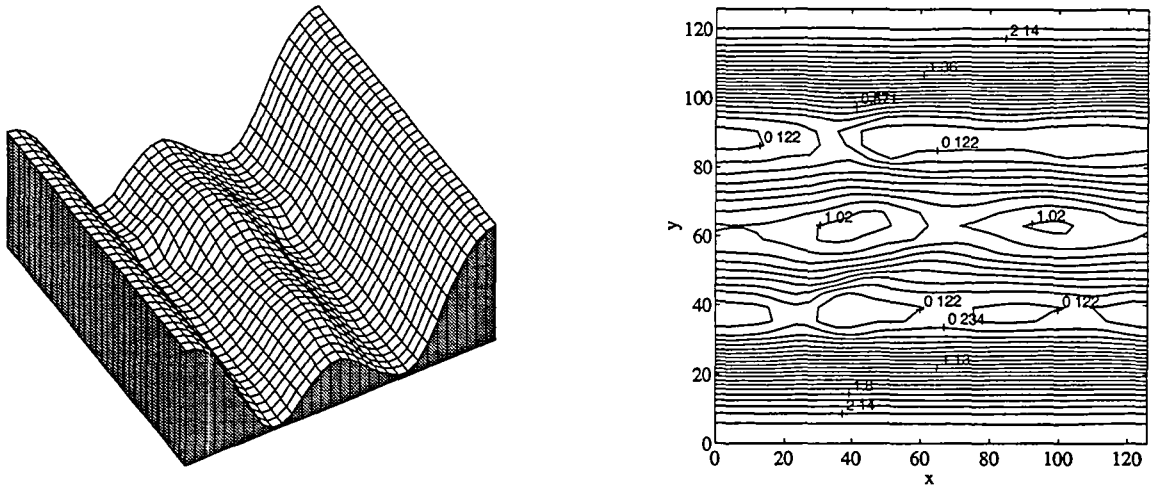

Figure 9 (e) t=1027

Figure 9: G=1,S=100,Bi=1,M=35,P=7,k_1=0.5, k_2=0.5, and β=90. The free-surface shape, contour plots of free-surface height from finite element simulation and spectral computation of long-wave evolution equation (Joo *et al.* 1995) are shown in order for (a) t=150, (b) t=300, (c) t=600, (d) t=970 and (e) t=1027. At t=1027, long-wave theory is no longer valid and only results from full-scale computation are shown.

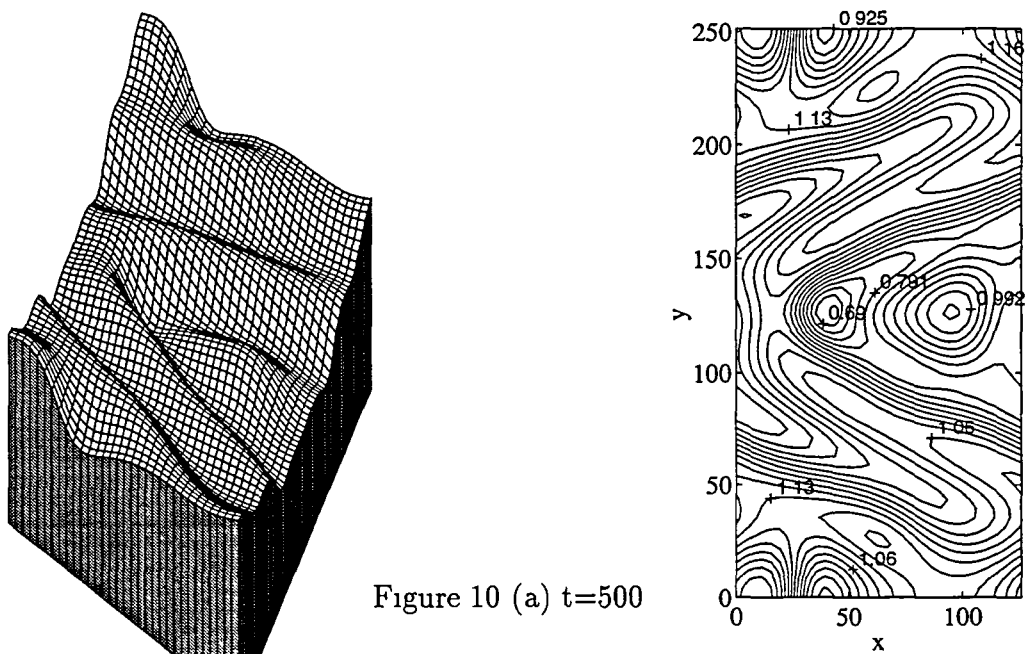

Figure 10 (a) t=500

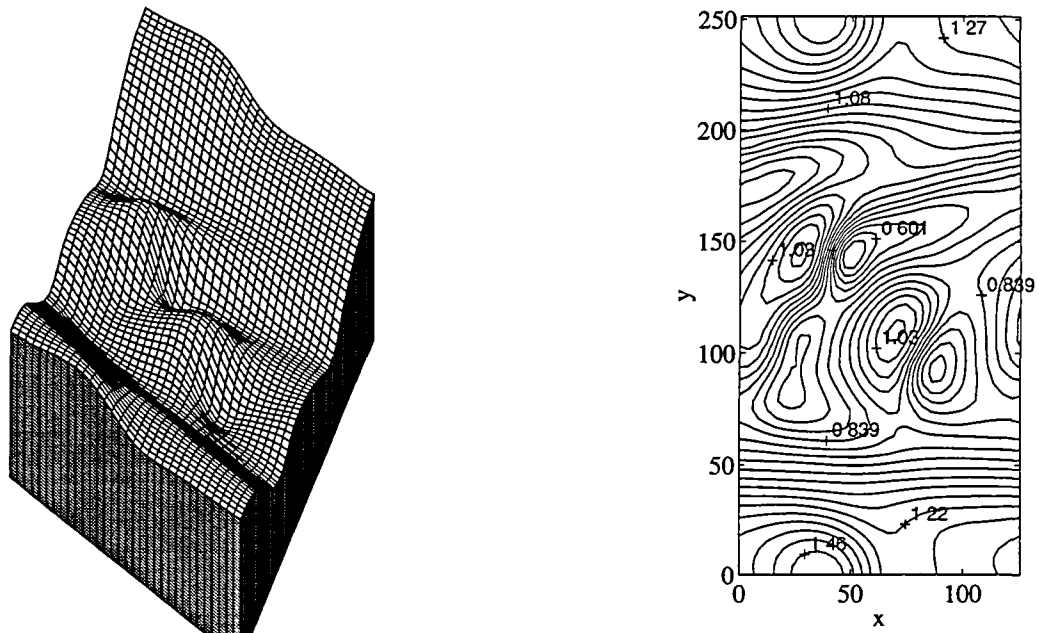

Figure 10 (b) t=1200

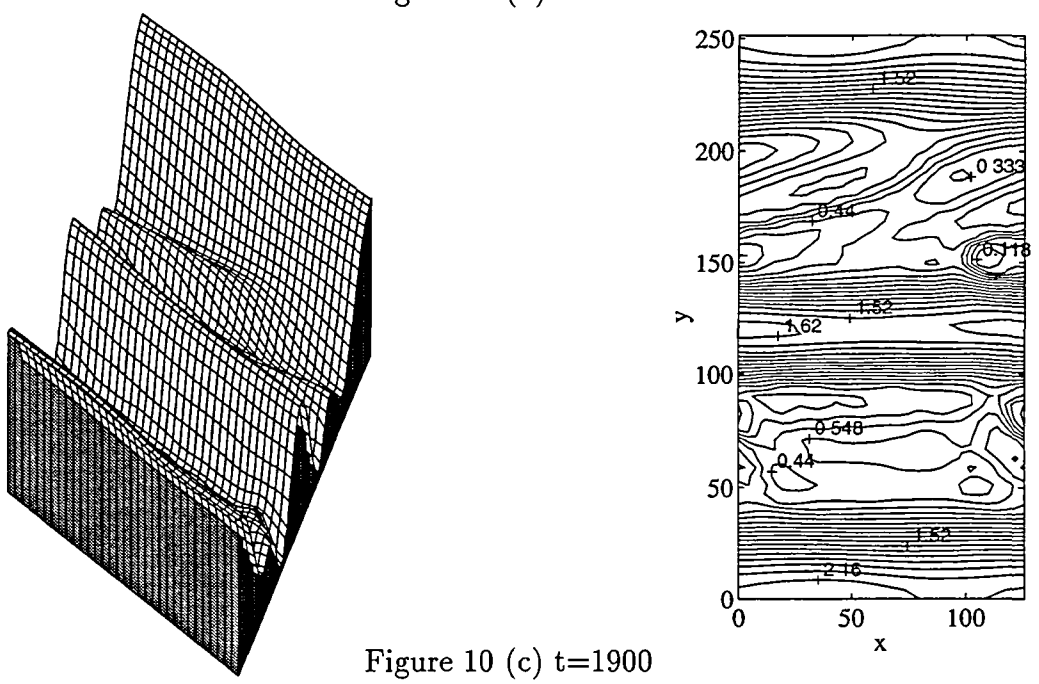

Figure 10 (c) t=1900

Figure 10: G=1,S=100,Bi=1,M=35,P=7,k_1=0.5, k_2=0.25, and β=90. The free-surface shape and contour plots of free-surface height from finite element simulation are shown for (a) t=500, (b) t=1200 and (c) t=1900.

5. CONCLUDING REMARKS

In this study, spontaneous rupture and rivulet formation of a thin film under combined thermocapillary and surface-wave instability is studied by solving the complete system of governing equations with fully nonlinear boundary conditions. Finite element method based on a projection scheme is used and the governing equations are solved in an Arbitrary Lagrangian Eulerian frame of reference. It is shown that spontaneous rupture always occurs by a "fingering" mechanism as predicted by long-wave theory. The growth of the fingers is isotropic when the film is horizontal. When we tilt the plate, surface-wave instability sets in. If thermocapillary is dominant, the film ruptures. On the other hand, if surface-wave instability is significant, the flow saturates into a steady wave form. Besides, the amount of heating, thickness of the film, angle of inclination and the amount of heat loss at the interface, the development of secondary flow shows strong dependency on the wavenumber of the imposed perturbation. In three-dimensional flow, when both thermocapillary and surface-wave instabilities are properly balanced, longitudinal rivulets aligned with the mean flow forms.

References

[1] P. Bach and J. Villadsen, "Simulation of the Vertical Flow of a Thin, Wavy Film Using a Finite Element Method", *International Journal for Heat and Mass Transfer*, **27**, 815-827, (1984).

[2] T.B. Benjamin, " Wave Formation in Laminar Flow Down an Inclined Plane", *Journal of Fluid Mechanics*, **2**, 554-557, (1957).

[3] D.J. Benny, "Long Waves on Liquid Films", *Journal of Mathematics and Physics*, **45**, 150-155 (1966).

[4] J.P. Burelbach, S.G. Bankoff and S H. Davis, "Nonlinear Stability of Evaporating/Condensing Liquid Films", *Journal of Fluid Mechanics*, **195**, 463-494, (1988).

[5] R.K.C Chan, "A Generalized Arbitrary Lagrangian Eulerian Method for Incompressible Flows with Sharp Interfaces", *Journal of Computational Physics*, **17**, 311-331, (1975).

[6] S. Chippada, "Numerical Study of Thin-Film Flows and Open Channel Flows", *Ph.D. Thesis*, Rice University, Houston, TX, USA, (1995).

[7] S. Chippada, T.C. Jue and B. Ramaswamy, "Finite Element Simulation of Combined Buoyancy and Thermocapillary Convection in Open Cavities", *International Journal of Numerical Methods in Engineering*, **38**, 335-351, (1995).

[8] A.J. Chorin, "Numerical Simulation of Navier-Stokes Equations", *Mathematics of Computation*, **22**, 745-762 (1968).

[9] J. Donea, "Arbitrary Lagrangian Eulerian Finite Element Methods", in *Computational Methods for Transient Analysis* (ed. T.B Belytschko and T.J.R. Hughes), 474-516, (1983)

[10] J. Donea, S. Giuliani and J.P. Halleux, "An Arbitrary Lagrangian Eulerian Finite Element Method for Transient Dynamics Fluid-Structure Interactions", *Computational Methods in Applied Mechanics and Engineering*, **30**, 53-73, (1982).

[11] D.A Goussis and R.E. Kelly, "On the Thermocapillary Instabilities in a Liquid Layer Heated from Below", *International Journal of Heat and Mass Transfer*, **33**, No. 10, 2237-2245 (1990).

[12] D.A. Goussis and R.E. Kelly, "Surface Waves and Thermocapillary Instabilities in a Liquid Film Flow", *Journal of Fluid Mechanics*, **223**, 25-45, (1991)

[13] D.E. Hartley and W. Murgatryod, "Criteria for the Breakup of Thin Liquid Layers Flowing Isothermally over Solid Surfaces", *International Journal of Heat and Mass Transfer*, **7**, 1003-1015, (1964).

[14] C.W. Hirt, A.A. Amsden and J.L. Cook, "An Arbitrary Lagrangian-Eulerian Computing Method for All Flow Speeds", *Journal of Computational Physics*, **14**, 227-253, (1974).

[15] L.W. Ho and A.T Patera, "A Legendre Spectral Element Method for Simulation of Unsteady Incompressible Viscous Free-Surface Flows", *Computational Methods in Applied Mechanics and Engineering*, **80**, 355-366 (1990).

[16] T.J.R. Hughes, W.K. Liu and T. Zimmerman, "The Lagrangian-Eulerian Finite Element Formulation for Incompressible Viscous Flow", *Computer Methods in Applied Mechanics and Engineering*, **29**, 329-349, (1981).

[17] S.W. Joo, S.H. Davis and S.G. Bankoff, "Long Wave Instabilities of Heated Falling Films", *Journal of Fluid Mechanics*, **230**, 177-146 (1991).

[18] S.W. Joo and S.H. Davis, "Instabilities of Three-Dimensional Viscous Falling Films", *Journal of Fluid Mechanics*, **242**, 529-547, (1992).

[19] S.W. Joo, S.H. Davis and S.G. Bankoff, "Two- and Three-dimensional Instabilities and Rupture of Thin Liquid Films Falling on Heated Inclined Plate", *Nuclear Engineering and Design*, **141**, 225-236 (1993).

[20] S.W. Joo, S.H. Davis and S.G. Bankoff, "A Mechanism for Rivulet Formation in Heated Falling Films", *submitted to Journal of Fluid Mechanics*, (1995).

[21] P.L Kapitza and S.P. Kapitza, "Wave Flow of Thin Layers of a Viscous Fluid:III, Experimental Study of Undulatory Flow Conditions", *Zh. Exp. Teor. Fiz*, **19**, 105,

(1949). Also in *Collected Papers of P.L. Kapitza* (ed.D.Ter Haar), **2**, 690-709, Pergamon, (1965).

[22] R.E. Kelly, S.H. Davis and D.A. Goussis, "On the Instability of Heated Film Flow with Variable Surface Tension", *Proceedings of 8th International Heat Transfer Conference*, 4, 1937-1942, (1986)

[23] H.S. Kheshgi and L E. Scriven, "Disturbed Film Flow on a Vertical Plate", *Physics of Fluids*, **30**, 990-997 (1987).

[24] S. Krishnamoorthy, B.Ramaswamy and S.W Joo, "Spontaneous Rupture of Thin Liquid Films Due to Thermocapillarity. A Full-Scale Direct Numerical Simulation", *Physics of Fluids*, (to appear), (1995).

[25] M. Lacroix and A. Garon, "Numerical Solution of Phase Change Problems: An Eulerian Lagrangian Approach", *Numerical Heat Transfer*, **19**, 57-78, (1992).

[26] S.P. Lin, "Stability of Liquid Flow Down a Heated Inclined Plane", *Letters in Heat and Mass Transfer*, **2**, 361, (1975).

[27] W.K. Liu, H. Chang, J. Chen and T. Belytschko, "Arbitrary Lagrangian Eulerian Petrov-Galerkin Finite Element Methods for Nonlinear Continua", *Computer Methods in Applied Mechanics and Engineering*, **68**, 259-310, (1988).

[28] N.T. Malamataris and T.C. Papanastasiou, "Unsteady Free Surface Flows on Truncated Domains", *Industrial Engineering and Chemical Research*, **30**, 2211-2219, (1991).

[29] J.R.A. Pearson, "On Convection Cells Induced By Surface Tension", *Journal of Fluid Mechanics*, **4**, 489-500 (1958).

[30] B. Ramaswamy, "Numerical Simulation of Unsteady Viscous Free Surface Flow", *Journal of Computational Physics*, **90**, 396-430 (1990).

[31] B. Ramaswamy and M. Kawahara, "Arbitrary Lagrangian-Eulerian Finite Element Method for Unsteady, Convective, Incompressible Viscous Free Surface Fluid Flow", *International Journal for Numerical Methods in Fluids*, **7**, 1053-1075, (1987).

[32] T.R. Salamon, R.C. Armstrong and R.A. Brown, "Traveling Waves on Vertical Films: Numerical Analysis by the Finite Element Method", *Physics of Fluids*, **6**, 2202-2220, (1994).

[33] L.E. Scriven and C.V. Sterling, "On Cellular Convection Driven Surface Tension Gradients: Effects of Mean Surface Tension and Surface Viscosity", *Journal of Fluid Mechanics*, **19**, 321-340 (1964).

[34] M.K. Smith and S.H. Davis, "Instabilities of Dynamic Thermocapillary Liquid Layers. Part 1. Convective Instabilities", *Journal of Fluid Mechanics*, **132**, 119-144 (1983).

[35] M.K. Smith and S.H. Davis, "Instabilities of Dynamic Thermocapillary Liquid Layers. Part 2. Surface-Wave Instabilities", *Journal of Fluid Mechanics*, **132**, 119-144 (1983).

[36] A. Soulaimani, M. Fortin, G. Dhatt and Y. Ouellet, "Finite Element Simulation of Two- and Three-Dimensional Free Surface Flows", *Computer Methods in Applied Mechanics and Engineering*, **86**, 265-296, (1991).

[37] C.S. Yih, "Stability of Laminar Parallel Flow with a Free Surface", *Proceeding of 2nd US National in Applied Mechanics*, ASME, 623, (1955).

[38] G.W. Young and S H. Davis, "Rivulet Instabilities", *Journal of Fluid Mechanics*, **176**, 1-31, (1987).

[39] N. Zuber and F.W. Staub, "Stability of Dry Patches Forming in Liquid Films Flowing over Heated Surface", *International Journal of Heat and Mass Transfer*, **9**, 897, (1966).

REPORT DOCUMENTATION PAGE

Form Approved
OMB No 0704-0188

1. AGENCY USE ONLY (*Leave blank*)	2. REPORT DATE	3. REPORT TYPE AND DATES COVERED
	September 1995	Final Contractor Report

4. TITLE AND SUBTITLE

Full-Scale Direct Numerical Simulation of Two- and Three-Dimensional Instabilities and Rivulet Formation in Heated Falling Films

5. FUNDING NUMBERS

WU–505–62–52
CTS–9408409

6. AUTHOR(S)

S. Krishnamoorthy, B. Ramaswamy, and S.W. Joo

7. PERFORMING ORGANIZATION NAME(S) AND ADDRESS(ES)

Rice University
Department of Mechanical Engineering and Materials Science
Houston, Texas 77251–1892

8. PERFORMING ORGANIZATION REPORT NUMBER

E–9917

9. SPONSORING/MONITORING AGENCY NAME(S) AND ADDRESS(ES)

National Aeronautics and Space Administration
Lewis Research Center
Cleveland, Ohio 44135–3191

10. SPONSORING/MONITORING AGENCY REPORT NUMBER

NASA CR–198403

11. SUPPLEMENTARY NOTES

S. Krishnamoorthy, Department of Mechanical Engineering and Materials Science, Rice University, Houston, Texas 77251–1892; B Ramaswamy, Department of Mechanical Engineering and Materials Science, Rice University, Houston, Texas 77251–1892 and Summer Faculty Fellow at Lewis Research Center; S.W. Joo, Wayne State University, Department of Mechanical Engineering, Detroit, Michigan 48202. Project Manager, D R. Reddy, Internal Fluid Mechanics Division, NASA Lewis Research Center, organization code 2610, (216) 433–8133.

12a. DISTRIBUTION/AVAILABILITY STATEMENT

Unclassified - Unlimited
Subject Categories 34 and 23

This publication is available from the NASA Center for Aerospace Information, (301) 621–0390

12b. DISTRIBUTION CODE

13. ABSTRACT (*Maximum 200 words*)

A thin film draining on an inclined plate has been studied numerically using finite element method. Three-dimensional governing equations of continuity, momentum and energy with a moving boundary are integrated in an Arbitrary Lagrangian Eulerian frame of reference. Kinematic equation is solved to precisely update interface location. Rivulet formation based on instability mechanism has been simulated using full-scale computation for the first time in the literature. Comparisons with long-wave theory are made to validate the numerical scheme. Detailed analysis of two- and three-dimensional nonlinear wave formation and spontaneous rupture forming rivulets under the influence of combined thermocapillary and surface-wave instabilities is performed

14. SUBJECT TERMS

Finite element method; ALE formulation; Spontaneous rupture; Rivulet; Long-wave theory

15. NUMBER OF PAGES

40

16. PRICE CODE

A03

17. SECURITY CLASSIFICATION OF REPORT	18. SECURITY CLASSIFICATION OF THIS PAGE	19 SECURITY CLASSIFICATION OF ABSTRACT	20 LIMITATION OF ABSTRACT
Unclassified	Unclassified	Unclassified	

End of Document